A Review of Imaging Methods for Prostate Cancer Detection

Libertas Academica
FREEDOM TO RESEARCH

Supplementary Issue: Image and Video Acquisition and Processing for Clinical Applications

Saradwata Sarkar[1] and Sudipta Das[2]

[1]Research and Development Division, Eigen, Grass Valley, CA, USA. [2]Department of Medicine, University of California, San Diego, CA, USA.

ABSTRACT: Imaging is playing an increasingly important role in the detection of prostate cancer (PCa). This review summarizes the key imaging modalities—multiparametric ultrasound (US), multiparametric magnetic resonance imaging (MRI), MRI–US fusion imaging, and positron emission tomography (PET) imaging—used in the diagnosis and localization of PCa. Emphasis is laid on the biological and functional characteristics of tumors that rationalize the use of a specific imaging technique. Changes to anatomical architecture of tissue can be detected by anatomical grayscale US and T2-weighted MRI. Tumors are known to progress through angiogenesis—a fact exploited by Doppler and contrast-enhanced US and dynamic contrast-enhanced MRI. The increased cellular density of tumors is targeted by elastography and diffusion-weighted MRI. PET imaging employs several different radionuclides to target the metabolic and cellular activities during tumor growth. Results from studies using these various imaging techniques are discussed and compared.

KEYWORDS: prostate cancer, multiparametric ultrasound imaging, multiparametric magnetic resonance imaging, positron emission tomography imaging

SUPPLEMENT: Image and Video Acquisition and Processing for Clinical Applications

CITATION: Sarkar and Das. A Review of Imaging Methods for Prostate Cancer Detection. *Biomedical Engineering and Computational Biology* 2016:7(S1) 1–15 doi:10.4137/BECB.S34255.

TYPE: Expert Review

RECEIVED: October 14, 2015. **RESUBMITTED:** January 7, 2016. **ACCEPTED FOR PUBLICATION:** January 11, 2016.

ACADEMIC EDITOR: Kayvan Najarian, Editor in Chief

PEER REVIEW: Three peer reviewers contributed to the peer review report. Reviewers' reports totaled 482 words, excluding any confidential comments to the academic editor.

FUNDING: Authors disclose no external funding sources.

COMPETING INTERESTS: Dr. Sarkar is employed at Eigen, and has a patent pending (62/238,836) for 3D multi parametric ultrasound imaging. Dr. Das discloses no competing interests.

CORRESPONDENCE: saradwataz@gmail.com

Paper subject to independent expert single-blind peer review. All editorial decisions made by independent academic editor. Upon submission manuscript was subject to anti-plagiarism scanning. Prior to publication all authors have given signed confirmation of agreement to article publication and compliance with all applicable ethical and legal requirements, including the accuracy of author and contributor information, disclosure of competing interests and funding sources, compliance with ethical requirements relating to human and animal study participants, and compliance with any copyright requirements of third parties. This journal is a member of the Committee on Publication Ethics (COPE).

Published by Libertas Academica. Learn more about this journal.

Introduction

The prostate is a walnut-sized male reproductive gland responsible for producing and secreting a thin, alkaline fluid that constitutes ~20–30% of the ejaculate. The smallest structural components of the gland—the acini—are surrounded by a basement membrane separating the secretory epithelial cells from surrounding structures. Proliferation of cells through the membrane causes prostate cancer (PCa). PCa is the second most frequently diagnosed cancer in men and the fifth leading cause of death worldwide.[1] In the USA alone, it is estimated that there will be 220,800 new PCa cases and 27,540 deaths due to PCa in 2015.[2]

Currently, the only definitive way to confirm PCa is through a prostate biopsy, wherein a physician samples prostate tissue from a few locations within the gland using a spring-loaded biopsy gun under image guidance (typically ultrasound [US] imaging). Early stage PCa is often asymptomatic, and a prostate biopsy is usually only indicated by one or more of the following factors: a family history of PCa, race (populations of African descent are found to be more genetically susceptible),[1] abnormal lumps within the prostate (usually detected by a physical digital rectal examination [DRE]), or an elevated serum prostate-specific antigen (PSA) level (the most widely used but controversial biomarker for PCa detection). Despite widespread efforts, it has been challenging to find a PSA cutoff that can reliably indicate the presence of cancer or the need for a biopsy. This is because serum PSA level is a gland-specific biomarker rather than being cancer-specific, ie, it is expressed in cancer cells as well as in hyperplastic cells of the prostate, especially benign prostatic hyperplasia (BPH).[3] The lack of reliable biomarkers necessitates the search for further avenues that can improve early detection, risk stratification, and disease monitoring for PCa patients. In the 2008 American Urological Association Whitmore lecture, Dr. Patrick Walsh mentioned:

> *The discovery that would have the greatest impact on our field would be the development of accurate imaging of tumor within the prostate.*

Rapid technological advances over the last few years have enabled the mainstream use of prostate imaging for the clinical management of PCa. Imaging modalities such as multiparametric ultrasound (mpUS), multiparametric magnetic resonance imaging (mpMRI), and nuclear imaging (positron emission tomography [PET]) are now being used for all facets of PCa—diagnosis and localization, whole-gland and focal therapy, staging, active surveillance, and recurrence monitoring. The goal of this review article is to discuss and

evaluate the important evolving role of multimodality imaging for biopsy guidance aimed at early initial detection of PCa or recurrence posttreatment. The review is organized based on the choice of major imaging modalities used to image PCa, ie, US, mpMRI, and PET imaging. Subsections within a specific modality discuss the various imaging techniques involved. Emphasis is made not only on the imaging techniques but also on the biological and functional characteristics of tumors that rationalize the use of these imaging methods.

Prostate Anatomy and Cancer

Before delving into the various modalities for prostate imaging, we will take a brief detour to comment on prostate anatomy, pathological grading, and treatment options for PCa to provide the context for our discussion in the subsequent sections.

Prostate anatomy. The prostate gland is located in the pelvis area and surrounded by the rectum posteriorly and the bladder superiorly. The gland itself surrounds part of the urethra. The part of the gland close to the bladder is referred to as the base, and the part close to the external urethral sphincter is referred to as the apex. Anatomically, the prostate is divided into four zones referred to as the McNeal zones— peripheral zone, or PZ, consisting of ~70% of glandular tissue; transition zone, or TZ, consisting of ~5% of glandular tissue; central zone, or CZ, consisting of ~25% of glandular tissue; and anterior fibromuscular stroma consisting of no glandular tissue (Fig. 1A). The relative incidence rates of PCa in these zones are 68% (PZ), 24% (TZ), and 8% (CZ).[4] These zones are easy to distinguish during image-guided interventional procedures of the prostate, such as prostate biopsy.

Pathological grading of PCa. As previously mentioned, the only way to confirm PCa currently is through an image-guided prostate biopsy procedure. The biopsy specimens obtained during the procedure are examined under a microscope to assign them a primary, secondary, and total Gleason score, which is a measure of cell differentiation and cancer aggressiveness (Fig. 1B). Specimens with a higher histopathological Gleason score (typically total Gleason score ≥ 7 or primary Gleason score ≥ 4) are indicative of worse prognosis, and such patients may be classified as harboring clinically significant cancer. On the other hand, clinically insignificant cancer (or cancer unlikely to cause mortality if left untreated) is widely considered as organ-confined, low-grade cancer (total Gleason score ≤ 6 with no Gleason component ≥ 4), with a gross tumor volume <0.5 cc.[5]

Treatment options for PCa. Patients diagnosed with clinically significant PCa often undergo radical prostatectomy (RP), whole-gland radiation therapy (RT), or hormonal therapy for the treatment of disease. Occasionally, such curative treatments may lead to side effects, such as urinary incontinence or impotence, which affect the quality of life of the patients. Recurrence, if any, of the disease posttreatment may be detected using a combination of serum PSA levels, imaging, and rebiopsy. Low-risk or clinically insignificant disease is often followed with active surveillance or watchful waiting programs, which may include image-based monitoring of disease progression

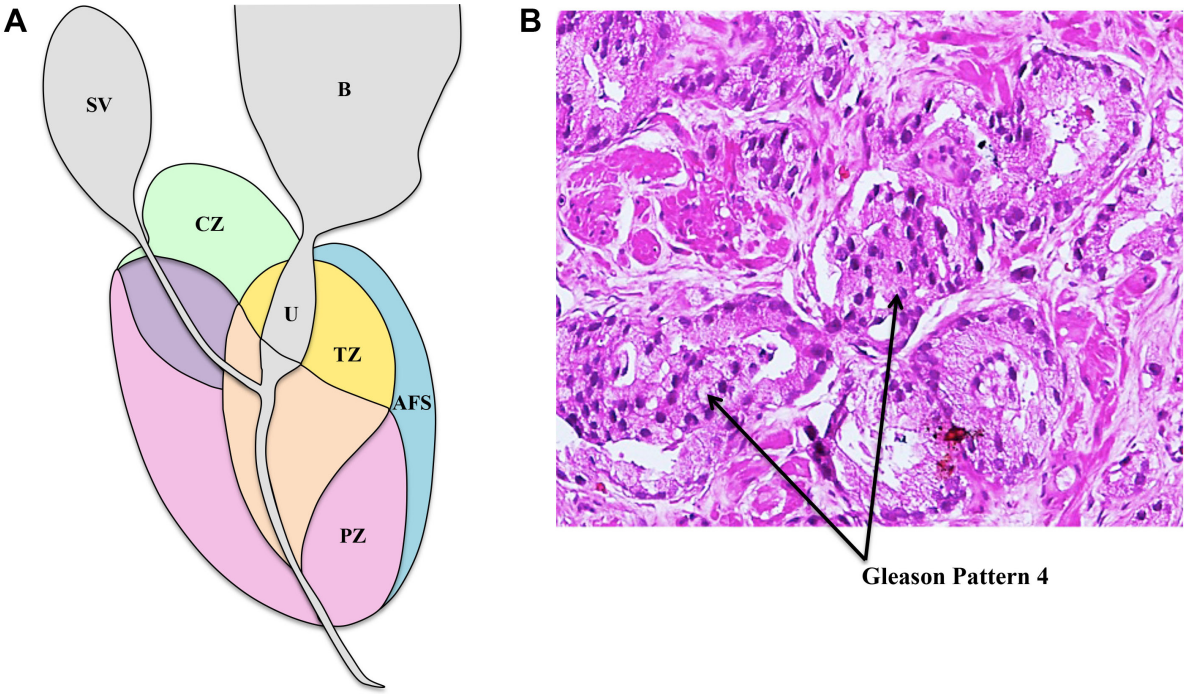

Figure 1. (**A**) Prostate zonal anatomy is depicted with the McNeal zones in sagittal view. SV: seminal vesicle (gray), B: bladder (gray), CZ: central zone (green), U: urethra (gray), TZ: transition zone (yellow), AFS: anterior fibromuscular stroma (blue), and PZ: peripheral zone (pink) (**B**) Immunostained biopsy specimen demonstrating Gleason pattern 4 adenocarcinoma of the prostate.

and/or multiple repeat biopsy sessions over a period of time. Recently, the viability of image-guided focal therapy or *male lumpectomy* is being explored as a treatment option for localized PCa and is likely to become more popular in the coming years.

Imaging Modalities

As previously mentioned, imaging has now become the mainstream choice for PCa detection and localization. Current major modalities for image-guided diagnosis of PCa include US-based imaging, mpMRI, mpMRI–US fusion imaging, and PET imaging. The choice of imaging modality is dictated by the biological behavior of the underlying tumor. In Figure 2, we provide a summary of the correspondence of the imaging modality to the characteristics of the imaged tumor. The individual correspondences are also elaborated in the following subsections. In Table 1, we provide a summary of the various imaging modalities in terms of their primary clinical usage and advantages and disadvantages.

US-based imaging. Anatomical US imaging is the oldest and most widely used technique to image PCa. Recently, the addition of US-based functional imaging techniques has created great interest in the research community. In the following subsections, we look at the various US imaging methods that are now leading to the development of an mpUS-based approach for PCa detection.

Grayscale or B-mode US. Grayscale or regular B-mode US is the most widely used imaging technique for detecting PCa. B-mode US allows the clear delineation of the zonal anatomy of the prostate—the outer PZ appears more echogenic than the inner CZ and TZ. In 1989, Hodge et al introduced the use of grayscale transrectal ultrasound (TRUS) imaging for guiding six biopsy needles through different parts of the prostate. When combined with the additional targeting of hypoechoic lesions (cancer tissue with cellular architecture defects appears less echogenic than normal tissue on grayscale US, as shown in Fig. 3), this technique formed the foundation of the *random and systematic* prostate biopsy that has been the standard of care since for detecting PCa.[6,7] Several biopsy optimization schemes have been discussed to improve the cancer detection rate using an extended-sextant 12-core biopsy that targets far lateral and apical PZ—the zone known to harbor the most cancer.[8]

Conventional B-mode anatomic US imaging for PCa has several limitations. Like cancerous tissue, several nonmalignant conditions of the prostate, such as prostatitis, inflammation,

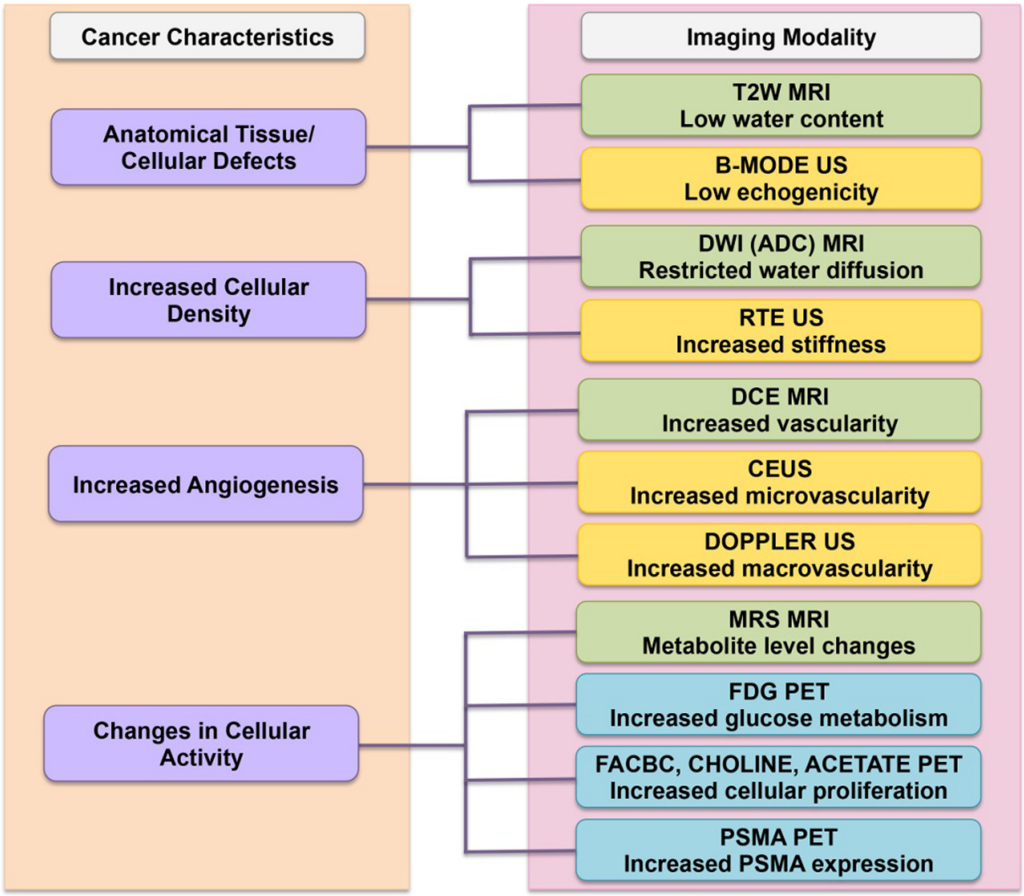

Figure 2. Correspondence of imaging modality to cancer characteristics. The left column shows the biological cancer characteristics and their correspondence to the choice of imaging modalities that exploit it are shown on the right. Specific imaging techniques are color coded based on the underlying major modality: US (yellow), MRI (green), and PET (blue).

Table 1. A summary of clinical usage, advantages, and disadvantages across imaging modalities for PCa imaging.

IMAGING MODALITY	CLINICAL USAGE	ADVANTAGES	DISADVANTAGES	FUTURE
Ultrasound-based	Initial detection and diagnosis	Office-based, widely available, inexpensive, real-time imaging	Limited tissue contrast between cancerous and benign tissue	mpUS-based approach (RTE, CEUS) may improve contrast
mpMRI-based	Initial diagnosis and recurrence, active surveillance, staging, metastatic involvement	Excellent tissue contrast for identification of clinically significant PCa	Expensive due to in-bore time, lack of real-time imaging, requires advanced training	Alternative in-bore options with real-time imaging being developed
mpMRI-ultrasound fusion-based	Initial detection and diagnosis, active surveillance	Office-based, combines multimodality information	Relatively costly, requires either fusion-device specific training or ample experience to perform cognitive fusion, registration errors during MRI-ultrasound fusion	Gaining popularity globally, but further improvements to minimize registration errors needed
PET-based	Staging, recurrence, metastatic spread	Offers ancillary information for tumor staging, characterization and metastatic involvement	Expensive, technological (e.g. attenuation correction) and/or clinical challenges (e.g. radiation exposure)	Development of specific radionuclides is an ongoing endeavor

and BPH, can appear hypoechoic on US imaging. Early stage carcinoma can also appear isoechoic due to the relatively higher proportion of normal glandular tissue.[9] Statistically, up to 60% of morphologically suspicious US lesions are known to be benign[10] and 21%–47% of tumors may be missed on an initial biopsy.[11,12] Additionally, the random and systematic sampling schemes are not tumor specific or patient specific and can lead to both incidental detection of clinically insignificant PCa (low-volume cancer with a total Gleason score of < 7)[12,13] and undergrading of the disease aggressiveness through insufficient sampling of the bulk of the tumor.[14]

Computer-aided US image analysis. PCa is characterized by changes in cellular structure that in turn affect the backscatter characteristics of US signal. This can then be used to classify malignant vs. benign tissue. Several commercially available devices have been developed for real-time, computer-based analysis of these US signals—for example, by using statistical analysis of raw US data (Prostate HistoScanning [PHS]) or artificial neural network analysis (ANNA) of digital B-mode US images (ANNA/computerized transrectal ultrasound [C-TRUS]).

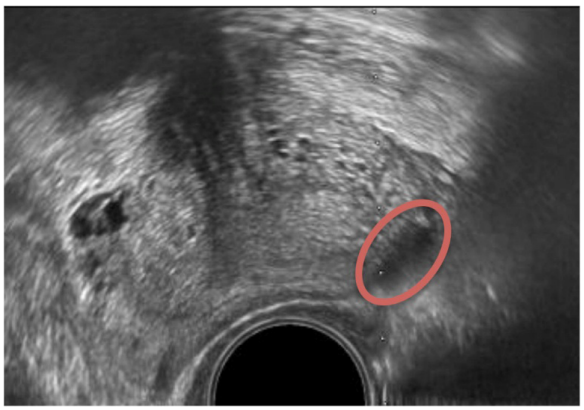

Figure 3. B-mode US image of the prostate depicting hypoechoic lesion (red oval).

Prostate HistoScanning. PHS is a technique that uses statistical analysis of raw backscattered US to pinpoint suspicious prostate lesions. An early study by Braeckman et al on 29 patients scheduled for RP showed the sensitivity, specificity, negative predictive value (NPV), and positive predictive value (PPV) to be 100%, 82%, 80%, and 100%, respectively, for lesions at least 0.5 mL in size.[15] In a study by Simmons et al on 27 patients, PHS was shown to have a sensitivity and specificity of 90% and 72%, respectively, for lesions at least 0.2 mL in size. The performance of PHS was worst in anterior regions of the prostate and best in mid-posterior sectors.[16] Macek et al found a sensitivity and specificity of 60% and 66%, respectively, in detecting lesions >0.1 cm^3 in 98 men.[17] Javed et al conducted three independent studies in a total of 105 men to gage the performance of PHS in routine clinical settings but found it to be unreliable. In these studies, the patients were examined using PHS before undergoing TRUS-guided biopsy (TGB; $n = 24$), transperineal template biopsy (TTB; $n = 57$), and RP ($n = 24$). The cancer detection rates for PHS vs. TGB and TTB were 38.1% vs. 62.5% and 13.4% vs. 54.4%, respectively. Moreover, no correlation was found between tumor volume estimates obtained from PHS and RP pathology.[18] Similarly, Schiffmann et al found no correlation between the tumor volumes found on RP and those found by PHS for 148 patients.[19] At this moment, the lack of robust, reproducible, clinical evidence affects the utility of this technique for PCa detection.[20]

Artificial neural net analysis/computerized transrectal ultrasound. The ANNA/C-TRUS system for PCa detection is based on ANNA of C-TRUS images to classify tissue regions as malignant or benign. Using this system, the physician performs a regular B-mode transrectal US examination of the prostate and sends the digital images to a central server that

performs ANNA of these images and returns them to the end user with potentially malignant regions highlighted. The user then guides his or her biopsies to these highlighted regions. The ANNA classifier was trained using the sets of correlated US images from RP specimens with known pathology.

In a study of 132 men with one to seven prior negative conventional grayscale US biopsies, the ANNA/C-TRUS system detected cancer in 50% of men. The historical detection rate of PCa in men with repeat biopsy using conventional US-guided systematic techniques is ~7%.[21] In another study of 75 biopsy naïve men, the ANNA/C-TRUS detected PCa in 41% of the cohort.[22] Strunk et al have also demonstrated that the combination of mpMRI and C-TRUS can improve PCa detection in high-risk patients.[23] The initial results using ANNA/C-TRUS are promising, and larger multicenter trials are needed to gage its true clinical efficacy.

Doppler US. PCa is often characterized by hyper vascularization and angiogenesis. In accordance with the Doppler effect, when US waves from a transducer strike the flowing red blood cells in blood vessels, there occurs a frequency shift of the reflected waves proportional to the velocity of the cells. This frequency shift is color overlaid on live B-mode US images and depicts the regions of increased perfusion, such as those characterized by tumors. The targeting of these regions of increased blood flow forms the crux of PCa detection using color Doppler ultrasound (CDU) imaging. Power Doppler ultrasound (PDU) imaging is another variant that displays the total integrated Doppler power in color. While the sense of direction of flow is lost using PDU imaging, it is more sensitive to perfusion than CDU, and hence, lower blood flow in smaller diameter blood vessels is potentially better detected using PDU imaging.

The performance of Doppler imaging for PCa detection varies. A study by Halpern et al on 62 patients comparing high-frequency CDU and PDU to random sextant biopsy showed no benefit of using Doppler imaging for PCa detection.[24] Okihara et al studied 107 men with high serum PSA levels using PDU imaging. PDU imaging indicated a lesion in 68 patients, and the final sensitivity, specificity, PPV, and NPV were 98%, 78%, 59%, and 99%, respectively.[25] Sauvain et al also showed a sensitivity and specificity of 45% and 74%, respectively, for detecting low-risk PCa in a cohort of 243 men using PDU imaging.[26]

The effectiveness of Doppler US imaging for PCa detection is affected by its limited resolution in detecting blood flow in any vessels <0.1 mm^9. Cancer growth is characterized by a dominant increase in the number of neo-microvessels that are often only 10–50 μm in diameter. As such Doppler imaging may only be effective in detecting increased blood flow in larger macrovessels that may be found in late-stage higher Gleason-grade tumors.

Contrast-enhanced ultrasound. As mentioned in the previous section, tumor growth and progression within the prostate is usually accompanied by angiogenesis and disorganized neovascularization that may significantly increase the microvascular density (MVD) of the affected region.[27] This increase in MVD is the target of contrast-enhanced ultrasound (CEUS) imaging. In CEUS imaging, highly echogenic gas-filled microbubbles are intravenously injected during the biopsy procedure.[28] These microbubbles are of a diameter comparable to the red blood cells and are easily able to flow as such (and be imaged) in the tumor microvasculature. This is the major advantage of CEUS in comparison to Doppler US imaging that is limited in its resolution to targeting the flow in larger macrovessels. Malignancy using CEUS is usually detected by asymmetrical rapid or focal enhancement.[29]

Quantitative analysis of CEUS involves investigating the time evolution of the US contrast agent concentration or by computing its dispersion kinetics while flowing through the microvasculature.[30–32] In a meta-analysis of 16 studies with 2624 patients, Li et al found a pooled sensitivity and specificity of 70% and 74%, respectively, for PCa detection using CEUS imaging.[33]

Real-time elastography. Most PCa tissue is known to be harder or stiffer than normal prostate tissue. The increased cellularity, increased micro vascularity, loss of glandular architecture, reduction in acinar area, and increased collagen deposition in the stroma surrounding cancer lead to increased stiffness of cancerous tissue in the prostate.[34] Actually, the physical DRE is predicated on the physician detecting harder or stiffer abnormal lumps of cancer tissue using the index finger to palpate the posterior PZ of the prostate. Real-time elastography (RTE) offers a more sophisticated and reliable whole-gland alternative for detecting these stiffer regions within the prostate gland. In RTE imaging, the physician induces a mechanical excitation in the prostate tissue and then images the response usually using real-time US. Techniques are classified by the method used for inducing the excitation and include strain elastography (SE), acoustic radiation force impulse (ARFI) imaging, and shear wave elastography (SWE).

Strain elastography. In SE, a US probe is used to create cyclical mechanical compressions/decompressions of prostate tissue. This creates a differential strain or deformation of the prostate tissue, which is coded to a color map and overlaid on the live B-mode US images. The live color map helps distinguish stiffer tissue from softer tissue and enables the physician to guide the biopsy needle to the stiffer locations (and hence more likely to be cancerous) in the prostate.

Zhang et al conducted a meta-analysis of seven studies that evaluated the performance of diagnostic SE with RP specimens as standard. In the combined population of 508 men, the pooled sensitivity and specificity were 72% and 76%, respectively.[35] SE has also been widely compared with MRI-guided biopsies. Aigner et al demonstrated similar sensitivity and NPV for strain RTE and T2-weighted MRI in an analysis of PZ lesions in 33 patients.[36] In a study by Pelzer et al, 50 patients with biopsy-proven cancer underwent strain RTE and mpMRI examinations to detect PCa were analyzed

retrospectively. The results were correlated with RP specimens. The sensitivity of strain RTE was higher than mpMRI (92% vs. 84%), although the authors commented that the MRI findings may have been confounded by the prior biopsies that causes hemorrhaging artifacts on MRI. Interestingly, strain RTE performed better in the dorsal and apical to the middle parts of the prostate and MRI performed better in the base and TZ.[37] In a cohort of 121 prior negative men undergoing fusion biopsies, Brock et al improved the specificity by using MRI/strain RTE fusion to target suspicious lesions. Sensitivity and specificity for MRI/strain RTE fusion were 77.8% and 77.3% vs. 74.1% and 62.9% for MRI alone, respectively.[38]

A major challenge of SE is that the free-hand compressions/decompressions using the endorectal US probe are operator dependent and require considerable expertise. To overcome this, Tsutsumi et al looked into using inflated balloons for applying more uniform compressions.[39] Another challenge of SE is that the interpretation of the live color maps is also operator dependent. The color maps are automatically scaled to the highest and lowest strains in a given 2D imaging plane, and it is challenging to get an absolute quantitative 3D threshold of stiffness that can distinguish malignant from benign tissue in the entire gland.[40]

Acoustic radiation force impulse imaging. ARFI imaging involves the delivery of short-duration (<1 millisecond) high intensity-focused US beams onto prostate tissue. A momentum transfer from the acoustic US waves to the propagating medium causes the generation of an acoustic radiation force that displaces tissue.[41] The displacement is then measured by the US probe. Just like in strain imaging, stiffer areas of the prostate, eg, tumors, displace less compared to normal soft tissue. This allows the physician to biopsy these regions when presented with a real-time color-coded map of displacements. The main advantage of ARFI over SE is that it is not dependent on manual free-hand compressions/decompressions of the prostate and hence requires less operator expertise.

Zhai et al[42] conducted a study on nine excised human prostate specimens and successfully distinguished the McNeal zones, BPH, calcifications, atrophy, and cancerous lesions within the prostates using ARFI imaging. They also reproduced this outcome in an in vivo study[43] of 19 patients prior to prostatectomy. However, in both studies, the ARFI pulses had limited depth penetration that affected anterior PCa detection.

Shear wave elastography. In SWE, acoustic radiation force is used to generate a shear wave in prostate tissue and the shear wave velocity is then measured. As shear wave velocity is proportional to the Young's modulus (a measure of stiffness expressed in kPa) of the tissue, a quantitative image of tissue stiffness can be created using SWE. Besides being quantitative, SWE imaging unlike SE does not require manual pressuring of the probe. Both these factors make SWE generalizable and less operator dependent.

In an initial SWE evaluation study of 53 men using a Young's modulus threshold of 37 kPa to differentiate benign vs. malignant tissue, Barr et al found a sensitivity, specificity, PPV, and NPV of 96%, 96%, 69%, and 100%, respectively.[44] In a real-time SWE study involving 1040 PZ sextants in 184 men, Correas et al found a sensitivity, specificity, PPV, and NPV of 96%, 85%, 48%, and 99%, respectively, using a threshold of 35 kPa.[45] Boehm et al established a cutoff of 50 kPa for 60 patients prior to prostatectomy using whole-gland SWE. They obtained a sensitivity, specificity, PPV, and NPV of 81%, 69%, 67%, and 82%, respectively.[46] Ahmad et al, in a study of 50 men, obtained sensitivity and specificity of ~90% each and suggested a relationship between increasing Young's modulus and increasing Gleason grade. However, the absolute stiffness values between benign and malignant tissue were considerably different than the other studies (75 kPa vs. 134 kPa, respectively).[47]

SWE imaging has certainly shown encouraging initial results, and several studies have demonstrated a significant difference between the Young's modulus of benign and malignant tissue. However, an absolute quantitative threshold to distinguish the two still remains to be determined.

Multiparametric US. All the abovementioned US-based imaging techniques exploit different biological characteristics of tumors, ie, increased vasculature, increased stiffness, etc. Recently, researchers have adopted a relatively mpUS approach that combines these functional techniques to improve the specificity of targeting. Aigner et al used RTE and CEUS to sample five targeted cores in 133 men. The overall cancer detection rate using the biparametric technique was 59.4%.[48] Xie et al combined the use of grayscale, Doppler, and CEUS imaging in 150 men to achieve an overall detection rate of 49%. The combination of the mpUS techniques detected more patients with PCa than grayscale ($P = 0.002$), power Doppler ($P = 0.001$), and grayscale plus power Doppler ($P = 0.031$).[49] Brock et al used RTE and CEUS for 86 patients and compared the pathology with the whole-mount sections. Using the combination of RTE and CEUS decreased the false positive rate from 35% to 10% and increased the PPV from 65% to 90%.[50] The mpUS techniques have shown great early promise, and larger patient cohort investigations in multicenter trials are needed for further development.

Multiparametric magnetic resonance imaging. Unlike US-based techniques that have usually been used independently of each other, MRI for PCa detection has largely followed a multiparametric approach. In such an approach, anatomical sequences (T2-weighted MRI) are combined with at least two functional MRI sequences (diffusion-weighted imaging [DWI] and dynamic contrast-enhanced imaging) for imaging the different biological characteristics of the tumor. For centers that have the expertise, MR spectroscopy (another functional MRI technique) may also be included in the acquisition protocol. When used in conjunction, these imaging techniques constitute the term mpMRI and help simultaneously assess different facets of the tumor.

T2-weighted imaging. High-resolution axial, sagittal, and coronal T2-weighted imaging (T2WI) sequences offer excellent soft tissue contrast and depiction of the zonal anatomy of the prostate (Fig. 4B). As such T2WI is best placed to identify defects in zonal anatomy, as exhibited by PCa cells (or to depict seminal vesicle invasion and extracapsular extension of disease). Normal PZ tissue is extremely water rich and composed of numerous ductal and acinar elements with sparsely interwoven smooth muscle. This gives it a bright or high-intensity appearance on T2-weighted images. On the other hand, PCa in the PZ appears as a rounded or ill-defined low-signal intensity focus (Fig. 4A) that contrasts with the high-signal intensity of the loosely packed normal PZ tissue.[51] The presence of a low-signal intensity focus in the PZ of T2-weighted images does not definitively indicate the presence of cancer because conditions such as prostatitis, atrophy, and prior biopsy-related hemorrhages may mimic this appearance as well. The normal TZ tissue has less water content, more compact smooth muscle, and sparser glandular components than the PZ and thus appears relatively darker on T2WI. PCa in the TZ appears as a homogeneous mass of low-signal intensity with indistinct margins. It is often hard to distinguish cancer from stromal BPH in the TZ, which may also appear as low-signal intensity due to its high muscular and fibrous contents.[51]

Diffusion-weighted imaging. PCa is typified by the regions of high cellular density or densely packed tumor cells. The high cellular density raises the intracellular/extracellular volume ratio of these regions that consequently restricts the random Brownian motion of water molecules in the extracellular space.[27] DWI is a functional technique that measures the random Brownian motion of water molecules.

For DWI, two or more sets of images are typically acquired by varying the magnetic field duration and strength (indicated by a *b*-value). Cancer appears as bright hyperintense regions on DW images because restricted water diffusion in these regions causes less signal loss. The multiple *b*-value DW images are also used to construct an Apparent Diffusion Coefficient (ADC) map where cancers appear as hypointense dark spots (Fig. 4C). ADC values have been found to predict cancer aggressiveness.[52] A recent topic of interest has been the computation of ultra-high *b*-value DWI (eg, $b = 2000$ seconds/mm^2; Fig. 4D) that may provide better determination of index lesions.[53,54]

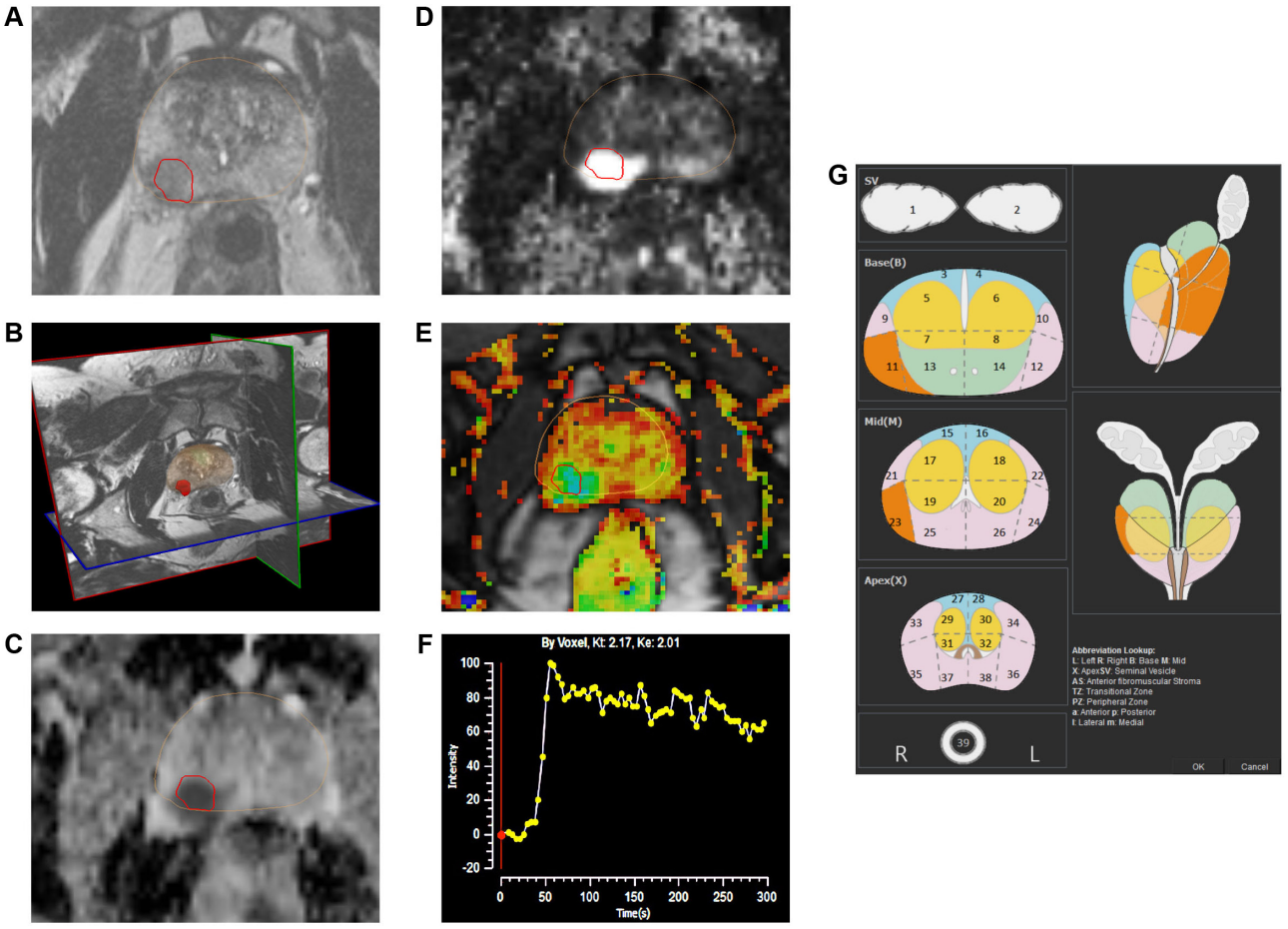

Figure 4. The mpMRI depiction of right posterolateral lesion: (**A**) axial T2-weighted image with lesion in red outline, (**B**) 3D T2-weighted view of prostate contour (brown) and lesion (red), (**C**) ADC image with lesion in red outline, (**D**) computed high *b*-value = 2000 seconds/mm^2 image with lesion in red outline, (**E**) dynamic contrast-enhanced pharmacokinetic map with lesion in red outline, (**F**) average time–signal intensity curve plot of the lesion, and (**G**) PIRADS version 2 location of lesion (orange).

Dynamic contrast-enhanced imaging. In dynamic contrast-enhanced MRI (DCE-MRI), 3D T1-weighted images are serially acquired before, during, and after intravenous injection of contrast media (typically low-molecular-weight Gadolinium chelates that rapidly diffuse in extravascular extracellular space). As we have previously discussed, aggressive tumors are known to promote the production of angiogenic factors that increase microvessel growth. The newly formed microvessels are typically disorganized and have weaker walls that make them more permeable.[55] As such PCa tissue often exhibits early enhancement on DCE-MR images due to tumor angiogenesis.

The DCE-MR images are typically analyzed for lesions (a) qualitatively, by a visual inspection of subtraction time points for potentially cancerous spots showing focal enhancement; (b) semiquantitatively, by time–signal intensity curve analysis (Fig. 4F) of suspicious voxels to determine parameters such as time-to-peak, wash-in slope, etc.; and/or (c) quantitatively, by using compartmental pharmacokinetic modeling that involves the use of contrast media concentration and an arterial input function to determine and generate color-coded maps for the rates of contrast agent wash-in (Ktrans) and wash-out (Kep) (Fig. 4E).

Magnetic resonance spectroscopic imaging. Magnetic resonance spectroscopic imaging (MRSI) is based on determining the cellular metabolite concentrations in prostate tissue. Healthy prostate tissue (especially in the PZ) has high levels of citrate. These levels are decreased in cancerous tissue. Moreover, the levels of choline markedly rise due to higher cellular density, cell membrane turnover, and phospholipid metabolism during PCa.[56] Thus, an elevated choline-to-citrate ratio forms the basis for distinguishing PCa tissue using MR spectroscopy. In practice, because the resonant peak of creatine is hard to distinguish from that of choline, the ratio of choline + creatine to citrate is typically used. MRSI has been shown by Turkbey et al to improve the predictive value of mpMRI-based PCa detection.[57] MRSI typically requires considerable technical expertise to perform and lengthens acquisition time. As such its clinical application for initial PCa diagnosis is currently limited. It is mostly used for staging and detecting radiotherapy recurrence.

mpMRI-based PCa detection and localization. The performance of mpMRI-based PCa detection has been widely successful. In a study of 143 men by Rais-Bahrami et al for PCa detection, it was found that biparametric MRI (T2WI + DWI) had an area under the curve (AUC) of 0.8 (which outperformed the AUCs of 0.66 and 0.74 for PSA level and PSA density, respectively).[58] Schoots et al conducted a meta-analysis of evidence for the diagnostic benefits of using mpMRI-targeted biopsies vs. systematic biopsies. The analysis included 16 studies with 1926 men and found that while both MRI-guided and TGBs had similar cancer detection rates, MRI-guided biopsies improved the detection of clinically significant cancer (91% vs. 76%) and lowered the detection of clinically insignificant cancer (44% vs. 83%) in comparison.[59] Panebianco et al conducted a randomized study on 1140 men, half of whom underwent regular TGBs and the other half underwent mpMRI plus TGBs. The detection rate was 38% in the first cohort and 72% in the second cohort. Moreover, none of the men who had a negative MRI had clinically significant cancer identified on saturation biopsies.[60] Other studies have demonstrated the utility of targeting MRI-suspicious lesions for all cohorts of patients: biopsy naïve,[61] prior negative,[62] and active surveillance.[63]

A critical component of mpMRI-based imaging for PCa detection is the quality of the scanning acquisition protocol and the accuracy of reading of the scans. Efforts are currently ongoing to standardize acquisition protocols and reading techniques for prostate mpMR images. In 2012, the European Society of Urogenital Radiology (ESUR) published the Prostate Imaging and Reporting Data System (PIRADS) in an effort to standardize the acquisition protocol and assessment of cancer suspicion level and location for lesions identified on mpMRI.[64] Some studies have shown a good correlation in the increase in PCa detection with increasing PIRADS suspicion level.[65–67] Recently, the American College of Radiology, ESUR, and AdMeTech foundation collaborated to upgrade this standard to PIRADS version 2, which among other changes also advocates the use of 39-region charts (Fig. 4G) to specify lesion locations.[68] According to the latest PIRADS version 2, DCE-MRI does not contribute to the overall assessment of suspicion level for lower grade (PIRADS levels 1 and 2) and higher grade lesions (PIRADS 4 or 5). For equivocal or moderate-grade PIRADS 3 lesions, a positive DCE-MRI enhances the suspicion score to PIRADS level 4. Hence, the consensus expert opinion currently considers diagnostic quality T2WI and DWI/ADC images to be the primary MRI sequences used for suspicion level assessment of lesions. However, DCE-MRI acquisition is still recommended so as not to miss small clinically significant cancers.

MRI–US fusion. This section discusses a new brand of PCa imaging that is based on a fusion of the US and MRI techniques previously discussed. The goal of this fusion imaging is to combine the best features of both US and MR imaging without sacrificing their individual diagnostic clinical utility.

The high sensitivity and specificity of mpMRI for clinically significant PCa detection has revolutionized the field of PCa diagnosis. Hambrock et al compared in-bore mpMRI-guided biopsies to 10-core systematic TRUS biopsies in men prior to RP. They found that MRI-guided biopsies significantly outperformed conventional grayscale TGBs in terms of PCa detection (88% vs. 55%; P-value < 0.001).[69] However, while accurate, the use of MRI alone to guide biopsies is expensive and impractical given the sheer volume of prostate biopsies that are performed each year (approximately a million in the US alone). Performing in-bore biopsies involves longer procedure durations due to the absence of real-time imaging, which often makes it uncomfortable for patients. In addition,

specialized equipment and needles are needed to avoid safety hazards due to the strong magnetic field. While alternative options allowing in-bore biopsies with real-time imaging and faster robotic needle placements are being developed, it is still a work in progress.[70,71] Regular grayscale US imaging, in contrast to in-bore MRI techniques, is relatively inexpensive and quick but may not have the diagnostic potency of MRI.

In recent years, a viable alternative to MRI-guided, in-bore, and regular TGBs has come to the forefront—mpMRI–US fusion-guided biopsies. In MRI–US fusion-guided procedures, the biopsy is performed as usual with regular live B-mode US in an outpatient office setting, which keeps the costs and procedure times relatively down. Prior to the procedure, however, an mpMRI pelvic examination of the patient is conducted to ascertain areas abnormal on MRI. These areas are then mapped onto the US images using image fusion or image registration techniques during the biopsy procedure for targeting. The image fusion between MRI and US images can be done cognitively or visually by an expert uroradiologist.[72] However, this is subjective and may require considerable expertise not usually available beyond large academic research centers. A more popular alternative now is to use one of the several regulatory-cleared, commercially marketed MRI–US fusion devices. The fusion platforms offer a less operator-dependent way to perform biopsies of virtual MRI targets using real-time US. The various platforms themselves differ in the mode of US acquisition (3D volumetric, 2D sweep, etc.), tracking mechanism (eg, electromagnetic and electromechanical) for biopsy targeting, route of biopsies (transrectal vs. transperineal), and image fusion technique (rigid vs. elastic). In addition to MRI/US fusion-based targeting guidance, most systems also offer the ability to archive biopsied locations with pathological grades. This has important implications for patients under active surveillance or focal therapy, as the critical component for the success of such programs is hinged on the accuracy of the recorded biopsy locations.

We will discuss here three widely studied fusion biopsy platforms—Artemis (Eigen), UroNav (Invivo/Philips), and Urostation (Koelis). Some other available platforms are BiopSee (MedCom), Virtual Navigator (Esaote), HI RVS (Hitachi), BioJet (GeoScan), Mona Lisa (Biobot Surgical Pte Ltd.), and LOGIQ 9 (GE Healthcare). For an analysis of the different fusion systems, the reader is referred to the comprehensive reviews by Le et al,[73] Gayet et al,[74] and Logan et al.[75]

Artemis. The Artemis system is manufactured by Eigen, USA. The system employs semirobotic mechanical stabilization of the TRUS probe during biopsy to minimize the effect of free-hand deformation. Prior to the procedure, the 3D mpMR images are analyzed using the ProFuse radiology software to annotate suspicious lesions. During the procedure, a 3D volumetric US acquisition is performed by a mechanical rotation of the TRUS probe. This 3D US volume is subsequently fused with the 3D MRI volume using rigid and elastic fusion (Fig. 5A and 5B). The rigid fusion aims to correct orientation differences between the 3D MRI and 3D US volumes, and the elastic fusion aims to account for the local shape deformations that occur between the volumes due to differences in patient orientation, bladder/rectal filling, and pressure of the endorectal coil or TRUS probe. The fusion process leads to the *transfer* of the virtual MRI lesion locations to the real-time TRUS images for targeting. Post fusion, the probe/needle guide assembly is moved to the lesion locations using a visual graphical interface based on electromechanical tracking and the shot locations recorded (Fig. 5C). In addition to MRI–US fusion-based targeting, the system also offers an automatic template distribution of the systematic, random biopsy cores based on the patient's prostate shape and volume.

In a study by Sonn et al on a mixed cohort of 171 men on active surveillance and prior negative biopsies, the Artemis system found cancer in 53% men. Fusion biopsy-guided cores were found to be three times more likely to find cancer than systematic random biopsies and also to find more clinically significant cancers ($P = 0.001$). The biopsy findings correlated with mpMRI suspicion level of the targeted lesions, and the cancer detection rate was 94% among men with the highest suspicion level on mpMRI.[76] In another study by Sonn et al on 105 prior negative men, 34% men were found to have PCa (the historical detection rates in the prior negative population is $< 20\%$[77]), of whom 72% had clinically significant disease. Sonn et al also found that fusion biopsies discovered 1.4 times

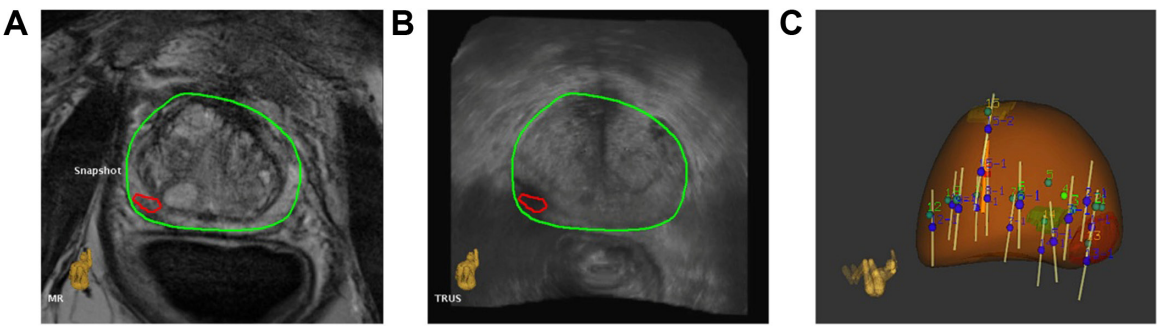

Figure 5. Depiction of MRI–US fusion. (**A**) and (**B**) show axial slices of fused MR and US images, respectively, with overlaid prostate contour (green) and lesion (red); (**C**) 3D prostate surface (brown) with archived biopsy core locations (white cylinders) after systematic and fusion biopsy.

more clinically significant cancers than systematic biopsies, but only 15% as many insignificant cancers.[78] Wysock et al compared Artemis-targeted fusion biopsies with expert cognitive fusion biopsies in a study of 125 men with 172 identified MRI-suspicious lesions. On a per target analysis, Artemis-targeted fusion biopsies detected 20.3% clinically significant cancers vs. 15.1% using cognitive targeting ($P = 0.0523$). Device-targeted biopsy was also found to be pathologically more informative than cognitive biopsies ($P = 0.0104$).[79]

UroNav. The UroNav platform was developed at the National Institutes of Health, Bethesda, USA, and is currently marketed by Invivo/Philips. The platform employs an external electromagnetic field generator to track and guide the needle biopsies transrectally. The 3D mpMR images are initially preprocessed, and the suspicious lesions are marked using the DynaCAD for Prostate platform. During the biopsy procedure, the 3D US volume is acquired using a 2D free-hand sweep from base to apex of the prostate. The fusion between the 3D MRI and 3D US images may be performed using a rigid technique that accounts for rotational and translational differences between the two images. The deformation between the US and MR 3D images can be adjusted by the user through visual adjustment of the US probe pressure on the prostate. After the fusion, the probe/needle assembly is maneuvered free-hand with electromagnetic guidance to the virtual MRI lesions for targeting.

In an initial study of 101 patients using the UroNav platform, Pinto et al found PCa in 28%, 69%, and 90% patients with low-, moderate-, and high-MRI suspicion levels, respectively ($P < 0.0001$).[80] In their study, the suspicion grade of a lesion was decided by the number of mpMRI sequences (T2WI, DCE, DWI, and MRSI) that detected that lesion as positive—low (2 or less), moderate (3), and high (4)—and denoted the likelihood of finding that lesion as cancerous upon biopsy. Vourganti et al found PCa in 37% of 195 men with prior negative biopsies and fusion-guided biopsies detected high-grade cancer in all men ($n = 21$), while systematic biopsies missed them in 12 patients.[81] In a large cohort study of 1003 men undergoing targeted and random systematic biopsies, Siddiqui et al found that targeted biopsy detected 30% more high-risk cancer ($P < 0.001$) and 17% fewer low-risk cancer ($P < 0.001$) than systematic biopsies.[82] Moreover, whole-gland pathology correlation for 170 men after RP indicated better predictive ability of targeted biopsies vs. systematic biopsies for distinguishing low-risk from high- and intermediate-risk cancer ($P < 0.05$).

Urostation. The Urostation platform was developed by Koelis, France, and differs from the Artemis and UroNav platforms in that the tracking is entirely software based, ie, it is neither electromechanical nor electromagnetic, but software image registration based. The system utilizes a 3D US probe to stitch together an initial 3D US volume. This 3D volume serves as the reference volume to register the subsequent biopsy locations. The 3D MR images are elastically fused with the 3D US volume to map the locations of the MRI lesions onto the US volume. Then, the US probe is maneuvered free-hand to the lesion locations for biopsy. Each biopsy location is retrospectively confirmed by acquiring another 3D volume at that location with the needle in place and then by elastically fusing it with the initial 3D reference volume.

Ukimura et al investigated the use of the Urostation platform for targeting MR-visible, hypoechoic, and isoechoic lesions on a phantom using fusion-guided biopsy. Overall, 84% of the fusion-guided biopsies successfully hit the lesions.[83] In a retrospective study of 90 patients, Rud et al demonstrated PCa detection rates of 10%, 27%, and 91% for low-, medium-, and high-MRI suspicion levels, respectively.[84] Mozer et al prospectively studied 152 men undergoing fusion and systematic biopsies and showed that the proportion of men detected with clinically significant cancer was higher using fusion biopsies than systematic biopsies ($P = 0.03$).[85]

Comments. As discussed earlier, mpMRI–US fusion imaging has produced impressive results using a variety of commercially marketed devices. The PCa detection rate has largely conformed to the suspicion grade on MRI. In the future, large multicentre/multidevice trials will likely help establish the real clinical utility of the different techniques.

PET imaging. PET involves the imaging of radiolabeled tracers inside the prostate after intravenous administration using gamma cameras. Currently, it is used in a limited capacity for the initial PCa diagnosis and more widely used for cancer staging, assessing biochemical failure after radiotherapy or metastasis involvement, eg, lymph nodes (Fig. 6). PET imaging critically highlights the metabolic, molecular, or cellular activity of prostate cells and is used in conjunction with anatomical imaging in the form of PET/MRI or PET/CT. Different methods of PET imaging are characterized by the choice of the chosen tracer and the targeted biological process, eg, metabolism, cellular proliferation, and receptor binding.

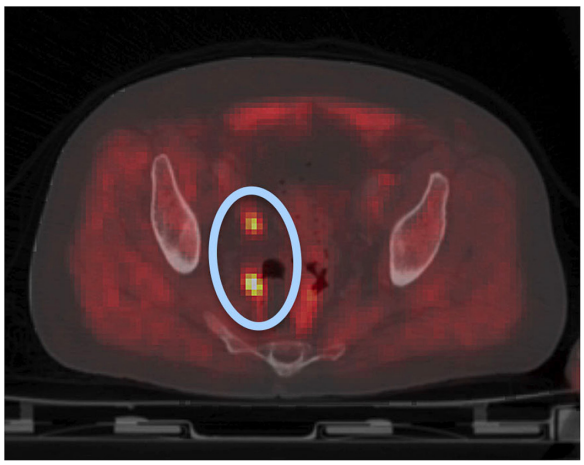

Figure 6. PET/CT image postprostatectomy depicting possible lymph node metastasis (blue oval with orange hot spots).

Metabolism targeted.

18F-fluorodeoxyglucose. The Warburg effect predicts increased glucose metabolism in malignant tissue using the glycolytic pathway as compared to normal tissue.[27] The most common radiotracer to monitor glucose metabolism in tumor cells is 18F-fluorodeoxyglucose (18F-FDG). However, 18F-FDG has been found to be not suitable for early or recurrent PCa detection because of relatively weak glucose metabolism in small, growing PCa cells and the close proximity of the prostate to the urinary bladder that confounds the uptake readings. The weak glucose metabolism results in a low uptake level of the radiotracer in tumor cells with significant overlap with normal tissue and BPH. Moreover, conditions such as prostatitis may even demonstrate higher FDG uptake than PCa cells.[86]

In a study by Yang et al on 100 patients with incidental FDG uptake, they found that the uptake in 20 patients was due to the presence of malignant lesions and the uptake in 80 patients was due to benign lesions.[87] However, FDG-PET imaging may continue to play an important role for detecting pelvic lymph node metastasis in patients with PSA relapse with negative whole-body bone scans. In an early study of 24 men with negative bone scans, Chang et al had found FDG-PET imaging to have a sensitivity, specificity, PPV, and NPV of 75%, 100%, 100%, and 67.7%, respectively, for detecting metastatic pelvic lymph nodes.[88]

Proliferation targeted.

1-Amino-3-fluorine-18-fluorocyclobutane-1-carboxylic acid. The radiotracer 1-amino-3-fluorine-18-fluorocyclobutane-1-carboxylic acid (18-F ACBC) exploits the fact that amino acid transport is upregulated in PCa cells. The low urinary excretion of this radiotracer also allows more accurate detection of 18-F ACBC uptake in malignant tumor cells.[89]

Schuster et al published that 18-F ACBC PET was more sensitive (89%) than US Food and Drug Administration (FDA)-approved [^{111}In]capromab pendetide single-photon emission computed tomography (SPECT)/computed tomography (CT) or ProstaScint (69%) in the detection of recurrent prostate carcinoma.[90] Schuster et al also studied the correlation between the uptake of anti-18-F ACBC with the histology of prostatectomy specimens of PCa patients and demonstrated that the maximum standardized uptake value significantly correlated with Gleason score at all time points ($P < 0.05$).[91] In a study by Turkbey et al, 21 patients underwent 18-F ACBC PET/CT and 3T mpMR imaging before prostatectomy. When compared to histopathologic findings, 18-F ACBC PET/CT had a sensitivity and specificity of 67% and 66%, respectively, for localizing PCa and a sensitivity of 90% for localizing dominant PCa. While the tracer uptake was higher for cancer tissue vs. normal tissue, there was overlap with BPH. The combined use of T2-weighted MRI with 18-F ACBC yielded a PPV of 82% for tumor localization, which was higher than either modality alone.[92]

11C-Choline and 18F-fluorocholine. The presence of PCa induces increased cellular membrane synthesis. Choline proliferates into the cells via choline transporters and is used for the synthesis of phosphatidylcholine, which is a prerequisite for cell membrane formation.[89,93] 11C-choline and 18F-fluorocholine (FCH) tracer imaging is predicated on the uptake of these radionuclides by index tumors.

Kwee et al performed FCH PET/CT in 50 patients with rising PSA levels at treatment (RP, RT, brachytherapy) follow-up. Abnormal tumor uptake was detected in 88% patients with a PSA level >1.1 ng/mL and in only 6% patients below this threshold value. Thus, they concluded that the effectiveness of FCH PET/CT in the detection of PCa recurrence was a function of PSA levels at the time of imaging.[94] Simone et al used a new FCH PET/CT imaging acquisition protocol with an early dynamic phase to gage biochemical recurrence in 146 patients with low PSA (<1 ng/mL). They found a sensitivity of 79% in this low PSA cohort, which suggests that FCH PET/CT may be a viable tool for an early detection of PCa recurrence.[95] In a study of 115 prostatectomy patients, Kitajima et al compared the efficacy of 11C-choline PET/CT vs. mpMRI. They found mpMRI to be superior to 11C-choline PET/CT for the diagnosis of recurrence (AUC 0.909 vs. 0.761, P-value < 0.01). However, the study also found 11C-choline PET/CT superior to mpMRI for the detection of lymph node metastasis.[96] A meta-analysis of 3167 patients from 47 different studies found 11C-choline or 18F-FCH PET/CT to be useful as a first imaging examination for patients with PCa and biochemical recurrence with PSA levels between 1 ng/mL and 50 ng/mL.[97]

11C-acetate. Like choline, acetate is a substrate needed for lipogenesis that is essential for increased cell membrane synthesis during PCa. The increased proliferation of acetate across cells also occurs through monocarboxylate transporters during PCa.[93]

Mohsen et al did a systematic review of the literature on the application of 11C-acetate PET imaging for PCa. In a pooled analysis of 23 studies, the sensitivity and specificity for primary tumor evaluation were 75.1% and 75.8%, respectively. For the detection of recurrence, sensitivity and specificity were 64% and 93%, respectively.[98] Buchegger et al compared FCH PET/CT with 11C-acetate PET/CT for the detection of recurrent PCa. Both tracers showed excellent concordance on a per-lesion and per-patient basis, suggesting equal efficacy for the detection of recurrence.[99]

Receptor targeted.

Prostate-specific membrane antigen. Prostate-specific membrane antigen (PSMA) is a membrane glycoprotein with an extensive extracellular domain, a transmembrane segment, and an intracellular domain.[100] PSMA is normally expressed in epithelial cells within the prostate and is strongly upregulated by all stages of PCa.[101] Increase in PSMA expression has been associated with tumor aggressiveness, metastasis, and disease recurrence,[102] thus providing a rational target for ligand–receptor-based imaging and therapy.

Several studies in animal models and pilot human studies have utilized radiolabeled antibodies/antibody fragments to

target intracellular or extracellular motifs of the antigen. These PSMA-based radiotracers include 64Cu-labeled aptamers and 11C-, 18F-, 68Ga-, and 86Y-labeled low-molecular-weight inhibitors of PSMA. In an initial clinical experience, 68Ga-labeled PSMA inhibitor has been suggested to better detect PCa relapse and metastasis as compared to 18F-choline.[103] ProstaScint scan was developed through indium-111 radiolabeling of the 7E11C5.3 antibody and remains the only FDA-approved PSMA agent to date.[89] ProstaScint scan acts by recognizing the intracellular portion of PSMA and offers the potential to characterize the nature of recurrence in patients with rising serum PSA levels after primary therapy.[104] Recently, in a study of 130 patients with intermediate- to high-risk PCa, preoperative lymph node staging with 68Ga-PSMA-PET proved to be superior to standard routine imaging using CT and MRI.[105] 68Ga-PSMA has also been recently shown to be useful for the restaging of PCa in patients being considered for salvage RT even at PSA levels <0.5 ng/mL.[106]

Comments. The experience with PET imaging for initial PCa detection is limited. However, PET imaging plays a critical role in detecting biochemical failure after PSA relapse.

Discussion

In 1989, the introduction of grayscale B-mode US imaging to guide transrectal biopsies of the prostate was an important breakthrough achieved by Hodge et al.[6] The use of transrectal US quickly replaced physical DRE as the choice for guiding needle biopsies for PCa diagnosis. Now, more than 25 years later, imaging is considered indispensable for all aspects of PCa management. In this review, we have summarized the role played by various imaging modalities such as US, MRI, and PET for PCa detection and localization. Regular B-mode or grayscale US remains, to date, the most widely used choice for PCa detection, but emerging scientific data are pushing other promising modalities to the forefront. While previously used only for staging and recurrence detection, clinics around the world are now increasingly utilizing mpMRI for PCa detection either in the form of direct in-bore MRI-guided biopsy or through MRI–US fusion-guided biopsy. Recently, CEUS and RTE have also emerged as promising US-guided techniques for PCa detection. This opens up the exciting potential for an integrated multimodality (mpUS and mpMRI) approach for PCa detection in the near future. PET imaging for PCa, in contrast to US and MRI, is used in a limited capacity for initial diagnosis and more widely used for cancer staging, assessing biochemical failure after radiotherapy or metastasis involvement.

The biological characteristics of the tumor and its evolutionary progression are a complex phenomenon. However, it is critical to understand the underlying processes that define tumor growth in order to make an optimal choice of imaging modality. In our discussion earlier, we have emphasized the tumor features that the imaging modalities seek to exploit and provided a summary in Figure 2.

With reference to US-based modalities, the simplest grayscale or B-mode US seek to image defects in zonal anatomy caused by prostatic tumors. As tumors are known to be angiogenic, Doppler US and CEUS attempt to image the macrovascularity and microvascularity of tumors, respectively. PCa tissue is often stiff and forms the basis for RTE of the prostate. The combined clinical deployment of these anatomical and functional US imaging techniques is referred to as mpUS or mpUS-based imaging of PCa. This is currently a topic of great interest to researchers around the world. If in future intraprocedure mpUS imaging and mpUS-based lesion assessment techniques can be standardized, it may well pave the way for very accurate and cost-effective office-based prostate biopsies.

mpMRI has arguably had the largest impact on PCa imaging in the last few years. Several studies have demonstrated that the use of direct MRI-guided biopsies or MRI–US fusion-guided biopsies improves the detection of clinically significant cancer and lowers the detection of clinically insignificant cancer. This has important implications for PCa management in that it prevents the underdetection of malignant disease and the overdetection (and often by consequence overtreatment) of indolent disease. mpMRI employs a multifaceted anatomical and functional approach to determine the presence or absence of PCa. T2-weighted images indicate suspicious anatomical variations in normal prostate tissue, which may be caused by cancer; DWI measures the restricted Brownian motion of water molecules caused by increased cellularity of tumors; and dynamic contrast-enhanced imaging exploits the enhanced vascularity of tumors caused by angiogenesis. MR spectroscopic imaging can also be used to gage abnormalities in the metabolite levels of prostate tissue caused by cancer cells.

While PET imaging is less used for initial PCa diagnosis, it plays an important role in the detection of biochemical relapse, PCa recurrence, and metastasis. Several radiolabeled tracers are in use for this purpose. PET is also typically combined with CT or MR for anatomical localization of the uptake hot spots of the radiotracers. The choice of the radiotracers themselves is determined by the biology of the tumor. The 18F-FDG tracer targets increased glucose metabolism of tumors, the 18-F ACBC-, choline-, and acetate-based tracers target molecules that are upregulated and proliferate during tumor growth, and PSMA-based tracers target ligand–receptor interactions in tumors with increased PSMA expression.

In summary, state-of-the-art imaging techniques have truly revolutionized the way we approach PCa management and more exciting research and innovations lie ahead of us in the future.

Conclusion

Imaging is playing an increasingly important role in the early detection and management of PCa. This review summarizes the key imaging modalities—mpUS, mpMRI, MRI–US

fusion imaging, and PET imaging—used in the diagnosis and localization of PCa. Emphasis is laid on the biological characteristics of tumors that rationalize the use of specific imaging techniques.

Author Contributions

Conceived the concepts: SS. Analyzed the data: SS. Wrote the first draft of the manuscript: SS. Contributed to the writing of the manuscript: SD. Agreed with the manuscript results and conclusions: SS and SD. Jointly developed the structure and arguments for the paper: SS and SD. Made critical revisions and approved the final version: SS and SD. All the authors reviewed and approved the final manuscript.

REFERENCES

1. Torre LA, Bray F, Siegel RL, Ferlay J, Lortet-Tieulent J, Jemal A. Global cancer statistics, 2012. *CA Cancer J Clin*. 2015;65(2):87–108.
2. Surveillance Epidemiology and End Results Program. *SEER Stat Fact Sheets: Prostate Cancer*. 2015. Available at: http://seer.cancer.gov/statfacts/html/prost.html
3. Botchorishvili G, Matikainen MP, Lilja H. Early prostate-specific antigen changes and the diagnosis and prognosis of prostate cancer. *Curr Opin Urol*. 2009; 19(3):221–226.
4. McNeal JE, Redwine EA, Freiha FS, Stamey TA. Zonal distribution of prostatic adenocarcinoma. Correlation with histologic pattern and direction of spread. *Am J Surg Pathol*. 1988;12(12):897–906.
5. Ohori M, Wheeler TM, Dunn JK, Stamey TA, Scardino PT. The pathological features and prognosis of prostate cancer detectable with current diagnostic tests. *J Urol*. 1994;152(5 pt 2):1714–1720.
6. Hodge KK, McNeal JE, Stamey TA. Ultrasound guided transrectal core biopsies of the palpably abnormal prostate. *J Urol*. 1989;142(1):66–70.
7. Hodge KK, McNeal JE, Terris MK, Stamey TA. Random systematic versus directed ultrasound guided transrectal core biopsies of the prostate. *J Urol*. 1989;142(1):71–74.
8. Bjurlin MA, Wysock JS, Taneja SS. Optimization of prostate biopsy: review of technique and complications. *Urol Clin North Am*. 2014;41(2):299–313.
9. Ukimura O, Faber K, Gill IS. Intraprostatic targeting. *Curr Opin Urol*. 2012;22(2): 97–103.
10. Loch T, Eppelmann U, Lehmann J, Wullich B, Loch A, Stockle M. Transrectal ultrasound guided biopsy of the prostate: random sextant versus biopsies of sonomorphologically suspicious lesions. *World J Urol*. 2004;22(5):357–360.
11. Singh H, Canto EI, Shariat SF, et al. Predictors of prostate cancer after initial negative systematic 12 core biopsy. *J Urol*. 2004;171(5):1850–1854.
12. Taira AV, Merrick GS, Galbreath RW, et al. Performance of transperineal template-guided mapping biopsy in detecting prostate cancer in the initial and repeat biopsy setting. *Prostate Cancer Prostatic Dis*. 2010;13(1):71–77.
13. Zaytoun OM, Moussa AS, Gao T, Fareed K, Jones JS. Office based transrectal saturation biopsy improves prostate cancer detection compared to extended biopsy in the repeat biopsy population. *J Urol*. 2011;186(3):850–854.
14. Isariyawongse BK, Sun L, Banez LL, et al. Significant discrepancies between diagnostic and pathologic Gleason sums in prostate cancer: the predictive role of age and prostate-specific antigen. *Urology*. 2008;72(4):882–886.
15. Braeckman J, Autier P, Soviany C, et al. The accuracy of transrectal ultrasonography supplemented with computer-aided ultrasonography for detecting small prostate cancers. *BJU Int*. 2008;102(11):1560–1565.
16. Simmons LA, Autier P, Zat'ura F, et al. Detection, localisation and characterisation of prostate cancer by prostate HistoScanning(TM). *BJU Int*. 2012;110(1): 28–35.
17. Macek P, Barret E, Sanchez-Salas R, et al. Prostate histoscanning in clinically localized biopsy proven prostate cancer: an accuracy study. *J Endourol*. 2014; 28(3):371–376.
18. Javed S, Chadwick E, Edwards AA, et al. Does prostate HistoScanning play a role in detecting prostate cancer in routine clinical practice? Results from three independent studies. *BJU Int*. 2014;114(4):541–548.
19. Schiffmann J, Fischer J, Tennstedt P, et al. Comparison of prostate cancer volume measured by HistoScanning and final histopathological results. *World J Urol*. 2014;32(4):939–944.
20. Schiffmann J, Manka L, Boehm K, et al. Controversial evidence for the use of HistoScanning in the detection of prostate cancer. *World J Urol*. 2015;33(12): 1993–1999.
21. Loch T. Computerized transrectal ultrasound (C-TRUS) of the prostate: detection of cancer in patients with multiple negative systematic random biopsies. *World J Urol*. 2007;25(4):375–380.
22. Grabski B, Baeurle L, Loch A, Wefer B, Paul U, Loch T. Computerized transrectal ultrasound of the prostate in a multicenter setup (C-TRUS-MS): detection of cancer after multiple negative systematic random and in primary biopsies. *World J Urol*. 2011;29(5):573–579.
23. Strunk T, Decker G, Willinek W, Mueller SC, Rogenhofer S. Combination of C-TRUS with multiparametric MRI: potential for improving detection of prostate cancer. *World J Urol*. 2014;32(2):335–339.
24. Halpern EJ, Frauscher F, Strup SE, Nazarian LN, O'Kane P, Gomella LG. Prostate: high-frequency Doppler US imaging for cancer detection. *Radiology*. 2002;225(1):71–77.
25. Okihara K, Kojima M, Nakanouchi T, Okada K, Miki T. Transrectal power Doppler imaging in the detection of prostate cancer. *BJU Int*. 2000;85(9):1053–1057.
26. Sauvain JL, Sauvain E, Rohmer P, et al. Value of transrectal power Doppler sonography in the detection of low-risk prostate cancers. *Diagn Interv Imaging*. 2013;94(1):60–67.
27. Russo G, Mischi M, Scheepens W, de la Rosette JJ, Wijkstra H. Angiogenesis in prostate cancer: onset, progression and imaging. *BJU Int*. 2012;110(11 pt C): E794–E808.
28. Postema A, Idzenga T, Mischi M, Frinking P, de la Rosette JJ, Wijkstra H. Ultrasound modalities and quantification: developments of multiparametric ultrasonography, a new modality to detect, localize and target prostatic tumors. *Curr Opin Urol*. 2015;25(3):191–197.
29. Postema A, Mischi M, de la Rosette JJ, Wijkstra H. Multiparametric ultrasound in the detection of prostate cancer: a systematic review. *World J Urol*. 2015; 33(11):1651–1659.
30. Postema AW, Frinking PJ, Smeenge M, et al. Dynamic contrast-enhanced ultrasound parametric imaging for the detection of prostate cancer. *BJU Int*. 2015 Mar 6. doi: 10.1111/bju.13116.
31. Mischi M, Wijkstra H. Contrast dispersion imaging for cancer localization. *Conf Proc IEEE Eng Med Biol Soc*. 2014;2014:4268–4271.
32. Schalk SG, Demi L, Smeenge M, et al. 4-D spatiotemporal analysis of ultrasound contrast agent dispersion for prostate cancer localization: a feasibility study. *IEEE Trans Ultrason Ferroelectr Freq Control*. 2015;62(5):839–851.
33. Li Y, Tang J, Fei X, Gao Y. Diagnostic performance of contrast enhanced ultrasound in patients with prostate cancer: a meta-analysis. *Acad Radiol*. 2013; 20(2):156–164.
34. Good DW, Stewart GD, Hammer S, et al. Elasticity as a biomarker for prostate cancer: a systematic review. *BJU Int*. 2014;113(4):523–534.
35. Zhang B, Ma X, Zhan W, et al. Real-time elastography in the diagnosis of patients suspected of having prostate cancer: a meta-analysis. *Ultrasound Med Biol*. 2014;40(7):1400–1407.
36. Aigner F, Pallwein L, Schocke M, et al. Comparison of real-time sonoelastography with T2-weighted endorectal magnetic resonance imaging for prostate cancer detection. *J Ultrasound Med*. 2011;30(5):643–649.
37. Pelzer AE, Heinzelbecker J, Weiss C, et al. Real-time sonoelastography compared to magnetic resonance imaging using four different modalities at 3.0 T in the detection of prostate cancer: strength and weaknesses. *Eur J Radiol*. 2013;82(5):814–821.
38. Brock M, Eggert T, Palisaar RJ, et al. Multiparametric ultrasound of the prostate: adding contrast enhanced ultrasound to real-time elastography to detect histopathologically confirmed cancer. *J Urol*. 2013;189(1):93–98.
39. Tsutsumi M, Miyagawa T, Matsumura T, et al. Real-time balloon inflation elastography for prostate cancer detection and initial evaluation of clinicopathologic analysis. *AJR Am J Roentgenol*. 2010;194(6):W471–W476.
40. Correas JM, Tissier AM, Khairoune A, Khoury G, Eiss D, Helenon O. Ultrasound elastography of the prostate: state of the art. *Diagn Interv Imaging*. 2013; 94(5):551–560.
41. Rosenzweig S, Bouchard R, Polascik T, Zhai L, Nightingale K. Advanced ultrasound: prostate elastography and photoacoustic imaging. In: Bard RL, Fütterer JJ, Sperling D, eds. *Image Guided Prostate Cancer Treatments*. Berlin: Springer; 2014: 31–45.
42. Zhai L, Madden J, Foo WC, et al. Acoustic radiation force impulse imaging of human prostates ex vivo. *Ultrasound Med Biol*. 2010;36(4):576–588.
43. Zhai L, Polascik TJ, Foo WC, et al. Acoustic radiation force impulse imaging of human prostates: initial in vivo demonstration. *Ultrasound Med Biol*. 2012; 38(1):50–61.
44. Barr RG, Memo R, Schaub CR. Shear wave ultrasound elastography of the prostate: initial results. *Ultrasound Q*. 2012;28(1):13–20.
45. Correas JM, Tissier AM, Khairoune A, et al. Prostate cancer: diagnostic performance of real-time shear-wave elastography. *Radiology*. 2015;275(1):280–289.
46. Boehm K, Salomon G, Beyer B, et al. Shear wave elastography for localization of prostate cancer lesions and assessment of elasticity thresholds: implications for targeted biopsies and active surveillance protocols. *J Urol*. 2015;193(3):794–800.
47. Ahmad S, Cao R, Varghese T, Bidaut L, Nabi G. Transrectal quantitative shear wave elastography in the detection and characterisation of prostate cancer. *Surg Endosc*. 2013;27(9):3280–3287.

48. Aigner F, Schafer G, Steiner E, et al. Value of enhanced transrectal ultrasound targeted biopsy for prostate cancer diagnosis: a retrospective data analysis. *World J Urol*. 2012;30(3):341–346.
49. Xie SW, Li HL, Du J, et al. Contrast-enhanced ultrasonography with contrast-tuned imaging technology for the detection of prostate cancer: comparison with conventional ultrasonography. *BJU Int*. 2012;109(11):1620–1626.
50. Brock M, Loppenberg B, Roghmann F, et al. Impact of real-time elastography on magnetic resonance imaging/ultrasound fusion guided biopsy in patients with prior negative prostate biopsies. *J Urol*. 2015;193(4):1191–1197.
51. Bhavsar A, Verma S. Anatomic imaging of the prostate. *Biomed Res Int*. 2014; 2014:9.
52. Verma S, Rajesh A, Morales H, et al. Assessment of aggressiveness of prostate cancer: correlation of apparent diffusion coefficient with histologic grade after radical prostatectomy. *AJR Am J Roentgenol*. 2011;196(2):374–381.
53. Rosenkrantz AB, Chandarana H, Hindman N, et al. Computed diffusion-weighted imaging of the prostate at 3 T: impact on image quality and tumour detection. *Eur Radiol*. 2013;23(11):3170–3177.
54. Blackledge MD, Leach MO, Collins DJ, Koh DM. Computed diffusion-weighted MR imaging may improve tumor detection. *Radiology*. 2011;261(2): 573–581.
55. Verma S, Turkbey B, Muradyan N, et al. Overview of dynamic contrast-enhanced MRI in prostate cancer diagnosis and management. *AJR Am J Roentgenol*. 2012;198(6):1277–1288.
56. Verma S, Rajesh A. A clinically relevant approach to imaging prostate cancer: review. *AJR Am J Roentgenol*. 2011;196(3 suppl):S1–S10.
57. Turkbey B, Pinto PA, Mani H, et al. Prostate cancer: value of multiparametric MR imaging at 3 T for detection—histopathologic correlation. *Radiology*. 2010;255(1):89–99.
58. Rais-Bahrami S, Siddiqui MM, Vourganti S, et al. Diagnostic value of biparametric magnetic resonance imaging (MRI) as an adjunct to prostate-specific antigen (PSA)-based detection of prostate cancer in men without prior biopsies. *BJU Int*. 2015;115(3):381–388.
59. Schoots IG, Roobol MJ, Nieboer D, Bangma CH, Steyerberg EW, Hunink MG. Magnetic resonance imaging-targeted biopsy may enhance the diagnostic accuracy of significant prostate cancer detection compared to standard transrectal ultrasound-guided biopsy: a systematic review and meta-analysis. *Eur Urol*. 2015; 68(3):438–450.
60. Panebianco V, Barchetti F, Sciarra A, et al. Multiparametric magnetic resonance imaging vs. standard care in men being evaluated for prostate cancer: a randomized study. *Urol Oncol*. 2015;33(1):.e11–.e17.
61. Peltier A, Aoun F, Lemort M, Kwizera F, Paesmans M, Van Velthoven R. MRI-targeted biopsies versus systematic transrectal ultrasound guided biopsies for the diagnosis of localized prostate cancer in biopsy naive men. *Biomed Res Int*. 2015;2015:571708.
62. Abdi H, Zargar H, Goldenberg SL, et al. Multiparametric magnetic resonance imaging-targeted biopsy for the detection of prostate cancer in patients with prior negative biopsy results. *Urol Oncol*. 2015;33(4):e161–e167.
63. Abdi H, Pourmalek F, Zargar H, et al. Multiparametric magnetic resonance imaging enhances detection of significant tumor in patients on active surveillance for prostate cancer. *Urology*. 2015;85(2):423–428.
64. Barentsz JO, Richenberg J, Clements R, et al. ESUR prostate MR guidelines 2012. *Eur Radiol*. 2012;22(4):746–757.
65. Baur AD, Maxeiner A, Franiel T, et al. Evaluation of the prostate imaging reporting and data system for the detection of prostate cancer by the results of targeted biopsy of the prostate. *Invest Radiol*. 2014;49(6):411–420.
66. Cash H, Maxeiner A, Stephan C, et al. The detection of significant prostate cancer is correlated with the Prostate Imaging Reporting and Data System (PI-RADS) in MRI/transrectal ultrasound fusion biopsy. *World J Urol*. 2015 Aug 21. doi: 10.1007/s00345-015-1671-8.
67. Hamoen EH, de Rooij M, Witjes JA, Barentsz JO, Rovers MM. Use of the prostate imaging reporting and data system (PI-RADS) for prostate cancer detection with multiparametric magnetic resonance imaging: a diagnostic meta-analysis. *Eur Urol*. 2015;67(6):1112–1121.
68. Weinreb JC, Barentsz JO, Choyke PL, et al. PI-RADS prostate imaging—reporting and data system: 2015, version 2. *Eur Urol*. 2016;69(1):16–40.
69. Hambrock T, Hoeks C, Hulsbergen-van de Kaa C, et al. Prospective assessment of prostate cancer aggressiveness using 3-T diffusion-weighted magnetic resonance imaging-guided biopsies versus a systematic 10-core transrectal ultrasound prostate biopsy cohort. *Eur Urol*. 2012;61(1):177–184.
70. Tokuda J, Tuncali K, Iordachita I, et al. In-bore setup and software for 3T MRI-guided transperineal prostate biopsy. *Phys Med Biol*. 2012;57(18):5823–5840.
71. Tilak G, Tuncali K, Song SE, et al. 3T MR-guided in-bore transperineal prostate biopsy: a comparison of robotic and manual needle-guidance templates. *J Magn Reson Imaging*. 2015;42(1):63–71.
72. Haffner J, Lemaitre L, Puech P, et al. Role of magnetic resonance imaging before initial biopsy: comparison of magnetic resonance imaging-targeted and systematic biopsy for significant prostate cancer detection. *BJU Int*. 2011;108(8 pt 2): E171–E178.
73. Le JD, Huang J, Marks LS. Targeted prostate biopsy: value of multiparametric magnetic resonance imaging in detection of localized cancer. *Asian J Androl*. 2014;16(4):522–529.
74. Gayet M, van der Aa A, Beerlage HP, Schrier BP, Mulders PF, Wijkstra H. The value of magnetic resonance imaging and ultrasonography (MRI/US)-fusion biopsy platforms in prostate cancer detection: a systematic review. *BJU Int*. 2015 Aug 3. doi: 10.1111/bju.13247.
75. Logan JK, Rais-Bahrami S, Turkbey B, et al. Current status of magnetic resonance imaging (MRI) and ultrasonography fusion software platforms for guidance of prostate biopsies. *BJU Int*. 2014;114(5):641–652.
76. Sonn GA, Natarajan S, Margolis DJ, et al. Targeted biopsy in the detection of prostate cancer using an office based magnetic resonance ultrasound fusion device. *J Urol*. 2013;189(1):86–91.
77. Keetch DW, Catalona WJ, Smith DS. Serial prostatic biopsies in men with persistently elevated serum prostate specific antigen values. *J Urol*. 1994;151(6): 1571–1574.
78. Sonn GA, Chang E, Natarajan S, et al. Value of targeted prostate biopsy using magnetic resonance-ultrasound fusion in men with prior negative biopsy and elevated prostate-specific antigen. *Eur Urol*. 2014;65(4):809–815.
79. Wysock JS, Rosenkrantz AB, Huang WC, et al. A prospective, blinded comparison of magnetic resonance (MR) imaging-ultrasound fusion and visual estimation in the performance of MR-targeted prostate biopsy: the PROFUS trial. *Eur Urol*. 2014;66(2):343–351.
80. Pinto PA, Chung PH, Rastinehad AR, et al. Magnetic resonance imaging/ultrasound fusion guided prostate biopsy improves cancer detection following transrectal ultrasound biopsy and correlates with multiparametric magnetic resonance imaging. *J Urol*. 2011;186(4):1281–1285.
81. Vourganti S, Rastinehad A, Yerram NK, et al. Multiparametric magnetic resonance imaging and ultrasound fusion biopsy detect prostate cancer in patients with prior negative transrectal ultrasound biopsies. *J Urol*. 2012;188(6):2152–2157.
82. Siddiqui MM, Rais-Bahrami S, Turkbey B, et al. Comparison of MR/ultrasound fusion-guided biopsy with ultrasound-guided biopsy for the diagnosis of prostate cancer. *JAMA*. 2015;313(4):390–397.
83. Ukimura O, Desai MM, Palmer S, et al. 3-Dimensional elastic registration system of prostate biopsy location by real-time 3-dimensional transrectal ultrasound guidance with magnetic resonance/transrectal ultrasound image fusion. *J Urol*. 2012;187(3):1080–1086.
84. Rud E, Baco E, Eggesbo HB. MRI and ultrasound-guided prostate biopsy using soft image fusion. *Anticancer Res*. 2012;32(8):3383–3389.
85. Mozer P, Roupret M, Le Cossec C, et al. First round of targeted biopsies using magnetic resonance imaging/ultrasonography fusion compared with conventional transrectal ultrasonography-guided biopsies for the diagnosis of localised prostate cancer. *BJU Int*. 2015;115(1):50–57.
86. Jadvar H. Prostate cancer: PET with 18F-FDG, 18F- or 11C-acetate, and 18F- or 11C-choline. *J Nucl Med*. 2011;52(1):81–89.
87. Yang Z, Hu S, Cheng J, et al. Prevalence and risk of cancer of incidental uptake in prostate identified by fluorine-18 fluorodeoxyglucose positron emission tomography/computed tomography. *Clin Imaging*. 2014;38(4):470–474.
88. Chang CH, Wu HC, Tsai JJ, Shen YY, Changlai SP, Kao A. Detecting metastatic pelvic lymph nodes by 18F-2-deoxyglucose positron emission tomography in patients with prostate-specific antigen relapse after treatment for localized prostate cancer. *Urol Int*. 2003;70(4):311–315.
89. Marko J, Gould CF, Bonavia GH, Wolfman DJ. State-of-the-art imaging of prostate cancer. *Urol Oncol*. 2015 Jun 15. pii: S1078-1439(15)00239-2. doi: 10.1016/j.urolonc.2015.05.015.
90. Schuster DM, Savir-Baruch B, Nieh PT, et al. Detection of recurrent prostate carcinoma with anti-1-amino-3-18F-fluorocyclobutane-1-carboxylic acid PET/CT and 111In-capromab pendetide SPECT/CT. *Radiology*. 2011;259(3):852–861.
91. Schuster DM, Taleghani PA, Nieh PT, et al. Characterization of primary prostate carcinoma by anti-1-amino-2-[(18)F]-fluorocyclobutane-1-carboxylic acid (anti-3-[(18)F] FACBC) uptake. *Am J Nucl Med Mol Imaging*. 2013;3(1): 85–96.
92. Turkbey B, Mena E, Shih J, et al. Localized prostate cancer detection with 18F FACBC PET/CT: comparison with MR imaging and histopathologic analysis. *Radiology*. 2014;270(3):849–856.
93. Jadvar H. Molecular imaging of prostate cancer with PET. *J Nucl Med*. 2013; 54(10):1685–1688.
94. Kwee SA, Coel MN, Lim J. Detection of recurrent prostate cancer with 18F-fluorocholine PET/CT in relation to PSA level at the time of imaging. *Ann Nucl Med*. 2012;26(6):501–507.
95. Simone G, Di Pierro GB, Papalia R, et al. Significant increase in detection of prostate cancer recurrence following radical prostatectomy with an early imaging acquisition protocol with (18)F-fluorocholine positron emission tomography/computed tomography. *World J Urol*. 2015;33(10):1511–1518.
96. Kitajima K, Murphy RC, Nathan MA, et al. Detection of recurrent prostate cancer after radical prostatectomy: comparison of 11C-choline PET/CT with pelvic multiparametric MR imaging with endorectal coil. *J Nucl Med*. 2014;55(2): 223–232.

97. von Eyben FE, Kairemo K. Meta-analysis of (11)C-choline and (18)F-choline PET/CT for management of patients with prostate cancer. *Nucl Med Commun*. 2014;35(3):221–230.
98. Mohsen B, Giorgio T, Rasoul ZS, et al. Application of C-11-acetate positron-emission tomography (PET) imaging in prostate cancer: systematic review and meta-analysis of the literature. *BJU Int*. 2013;112(8):1062–1072.
99. Buchegger F, Garibotto V, Zilli T, et al. First imaging results of an intraindividual comparison of (11)C-acetate and (18)F-fluorocholine PET/CT in patients with prostate cancer at early biochemical first or second relapse after prostatectomy or radiotherapy. *Eur J Nucl Med Mol Imaging*. 2014;41(1):68–78.
100. Ghosh A, Heston WD. Tumor target prostate specific membrane antigen (PSMA) and its regulation in prostate cancer. *J Cell Biochem*. 2004;91(3):528–539.
101. Bouchelouche K, Turkbey B, Choyke PL. Advances in imaging modalities in prostate cancer. *Curr Opin Oncol*. 2015;27(3):224–231.
102. Ross JS, Sheehan CE, Fisher HA, et al. Correlation of primary tumor prostate-specific membrane antigen expression with disease recurrence in prostate cancer. *Clin Cancer Res*. 2003;9(17):6357–6362.
103. Afshar-Oromieh A, Zechmann CM, Malcher A, et al. Comparison of PET imaging with a (68)Ga-labelled PSMA ligand and (18)F-choline-based PET/CT for the diagnosis of recurrent prostate cancer. *Eur J Nucl Med Mol Imaging*. 2014;41(1):11–20.
104. Taneja SS. ProstaScint(R) scan: contemporary use in clinical practice. *Rev Urol*. 2004;6(suppl 10):S19–S28.
105. Maurer T, Gschwend JE, Rauscher I, et al. Diagnostic Efficacy of Gallium-PSMA-PET compared to Conventional Imaging in Lymph Node Staging of of 130 consecutive Patients with Intermediate to High-Risk Prostate Cancer. *J Urol*. 2015 Dec 9. pii: S0022-5347(15)05397-5. doi: 10.1016/j.juro.2015.12.025.
106. van Leeuwen PJ, Stricker P, Hruby G, et al. 68Ga-PSMA has high detection rate of prostate cancer recurrence outside the prostatic fossa in patients being considered for salvage radiation treatment. *BJU Int*. 2015 Dec 18. doi: 10.1111/bju.13397.